American Journal of Materials Synthesis and Processing
2017; 2(6): 97-102
http://www.sciencepublishinggroup.com/j/ajmsp
doi: 10.11648/j.ajmsp.20170206.15
ISSN: 2575-2154 (Print); ISSN: 2575-1530 (Online)

PEG-200 Assisted Sonochemical Synthesis of Cerium (Ce^{3+}) Doped Copper Oxide (CuO) Nano-Composites and Their Photocatalytic Activities

Sonali P. Chaudhari[1], Anjali B. Bodade[1], Prashant D. Jolhe[2], Satish P. Meshram[1, *], Gajanan N. Chaudhari[1, *]

[1]Nano Technology Research Laboratory, Department of Chemistry, Shri Shivaji Science College, Amravati, India

[2]Department of Biotechnology, Sinhgad College of Engineering, Savitribai Phule Pune University, Pune, India

Email address:

gnchaudhari@gmail.com (G. N. Chaudhari), satishmeshram99@gmail.com (S. P. Meshram)

[*]Corresponding author

To cite this article:

Sonali P. Chaudhari, Anjali B. Bodade, Prashant D. Jolhe, Satish P. Meshram, Gajanan N. Chaudhari. PEG-200 Assisted Sonochemical Synthesis of Cerium (Ce^{3+}) Doped Copper Oxide (CuO) Nano-Composites and Their Photocatalytic Activities. *American Journal of Materials Synthesis and Processing*. Vol. 2, No. 6, 2017, pp. 97-102. doi: 10.11648/j.ajmsp.20170206.15

Received: September 24, 2017; **Accepted**: October 18, 2017; **Published**: December 8, 2017

Abstract: CuO nanocomposites with different Ce^{3+} doping concentrations (0, 0.5, 1.0, 1.5, 3.0 and 5.0 mol.%) were synthesized by PEG-200 assisted facile sonochemical method. The as-synthesized composites were characterized by X-ray diffraction (XRD), field emission scanning electron microscopy (FESEM) and UV-visible absorption spectroscopy. Further, these composites were evaluated for photodegradation activities towards MB dye under sunlight irradiation. The XRD results demonstrated that CuO nanocomposites exhibits monoclinic phase and the crystallinity decreases with increasing Ce^{3+} doping concentration. The as-synthesized nanocomposites exhibited vesicular morphology with diameters ranging from 50 to 100nm. UV-visible absorption spectra results demonstrated that these nanocomposites exhibit strong absorption in the visible region and the absorption intensity increases with increasing Ce^{3+} doping concentration. The photocatalytic experiments using as-synthesized nanocomposites for degradation of Methylene blue (MB) dye revealed that, compared to undoped CuO; Ce^{3+} doped CuO nanocomposites exhibited improved photodegradation ability. The photodegradation rate was maximum for 3.0 mol% Ce^{3+} doped CuO which showed 98% degradation within 180 mins under sunlight irradiation. Recycling experiments demonstrated good stability of as-synthesized nanocomposites even after threere cycles.

Keywords: Ce Doped CuO, Sonochemical, Photocatalysis, Methylene Blue

1. Introduction

Usual nondestructive nature towards target contaminant associated with the traditional wastewater treatment technologies have led to lose their importance. Additionally, these traditional techniques such as ultra-filtration, precipitation and adsorption generate secondary pollutants by just transforming contaminants from water to other phases [1-6]. Recently, advanced oxidation processes (AOP's) have emerged as a potential technique capable of destroying the wide range of organic contaminants [7-12]. Comparatively, the greater popularity of this technique is due to its better efficiency and employment of non-toxic, cost-effective and readily available semiconductor photocatalysts.

Among various semiconductor photocatalysts employed in photocatalysis, TiO_2 and ZnO are widely explored and highlighted by various researchers [13]. However, the use of these materials still possesses some drawbacks such as TiO_2 can be utilized under UV light only and the ZnO exhibits low quantum efficiency due to very fast recombination. Since, CuO is a low cost and can be a good alternative to TiO_2 and ZnO; recently researchers are trying to explore possibility of employing CuO based materials for photocatalytic applications. CuO is *p*-type semiconductor having 1.2eV bandgap [14]. A wide range of applications of CuO in lithium ion batteries, supercapacitors, sensors, photodetectors, solarcells, heterogeneous catalysts, magnetic storage media

and field emitters etc have demonstrated its importance in scientific and industrial research both [15-18].

As far as utilization of CuO based materials for photocatalytic application is concerned, reported literature suggests that most of the time CuO has been utilized along with H_2O_2 to have desired photocatalytic activity [19-21]. It has been reported that, photoactivity of a semiconductor photocatalyst can be well improved by doping with certain cation [22]. In this scenario, various metal cation doped CuO nanomaterials are reported previously eg. S. G. Yang *et. al.* And R. A. Borzi *et. al.* Have investigated Zn and Mn doped CuO nanomaterials for ferromagnetic properties [23, 24]. Increased visible light absorption of CuO upon doping with Ag was reported by S. Manna *et. al.* [25]. Y. X. Li *et. al.* Investigated the room temperature ferromagnetic properties of Fe doped CuO [26]. M. Chuai *et. al.* Studied ferromagnetic properties of Ce doped CuO dilute magnetic semiconductors [27]. As can be seen from the extensive literature search, there are very less reports on synthesis of Ce doped CuO nanomaterials and their possible application in photocatalysis.

Considering above discussion, herein present study we are reporting PEG-200 assisted facile sonochemical method for synthesis of undoped and different mol% Cerium (Ce^{3+}) doped CuO nanocomposites. The as-synthesized nanocomposites were characterized by XRD, FESEM and UV-visible absorption spectroscopy and were further tested for sunlight mediated dye degradation of MB dye.

2. Experimental

2.1. Materials and Method

0, 0.5, 1.0, 1.5, 3.0 and 5.0% molar ratios Ce doped CuO nanocomposites were prepared by facile sonochemical method using copper acetate ($Cu(OAc)_2{\cdot}6H_2O$) as substrate, cerium nitrate ($Ce(NO_3)_3{\cdot}6H_2O$) as dopant source and PEG-200 (avg. mol. wt. 190-210) as structure directing agent. All the chemicals were of analytical grade and were purchased from Loba Chemie.

In a typical experiment; 0.02 mol copper acetate and 0-5.0 mol.% cerium nitrate were dissolved in 75 ml double distilled water premixed with 5% PEG-200. Subsequently, 0.2 M NaOH was slowly added into the solution till attainment of pH 10-11. The as-formed grey colored suspensions were then ultrasonically treated for 01h using sonicator probe at amplitude 35% and energy 40 kW. During sonication, the probe was operated 5 sec pulse ON and 2 sec pulse OFF. Post reaction, the precipitate was centrifuged, washed with distilled water and ethanol several times and finally dried in oven at 60°C for 24h.

2.2. Characterization

Rigaku Miniflex X-ray diffractometer with CuKα irradiation operated at λ=1.5406Å was employed for X-ray diffraction (XRD) analysis of as-synthesized samples. The surface morphology of as-synthesized samples was analyzed using a JEOL-JSM 6700F field-emission scanning electron microscope. For UV–visible absorption spectra analysis JASCOV-570 spectrophotometer was employed by transferring certain volume of ZnO suspension in a quartz cuvette.

2.3. Photocatalytic Activities

Photocatalysis experiments were carried out in 250 ml pyrex beaker under sunlight irradiations using as-synthesized catalysts. Prior to sun-light irradiation, adsorption-desorption equilibrium with MB dye molecules was ensured by agitating the suspension in dark for 30 mins. The extent of MB dye removal was analyzed by measuring changes in absorbance at 663nm.

3. Results and Discussions

3.1. XRDAnalysis

X-ray diffraction patterns of CuO and Ce^{3+} doped CuO with variable cerium contents are shown in Figure 1. All the diffraction peaks match to standard data for monoclinic CuO structure (JCPDS Card. No.05-0661) [28]. The diffraction peaks appearing at 2θ=32.5, 35.6, 38.7, 48.8, 53.4, 58.3, 61.6, 66.2, 68.1, 72.4 and 75.1° corresponds to (110), (002), (-111), (-112), (112), (020), (202), (022), (-311), (220) and (004) diffraction planes of monoclinic CuO. Beyond these peaks, no additional peaks related to Ce or cerium oxides were detected within the detection limit of XRD instrument, which further suggests that Ce^{3+} ions are entered into the CuO lattices by substituting Cu^{2+} or existed in amorphous forms. However, the incorporation of Ce^{3+} ions into CuO lattice has no effect on the crystal structure.

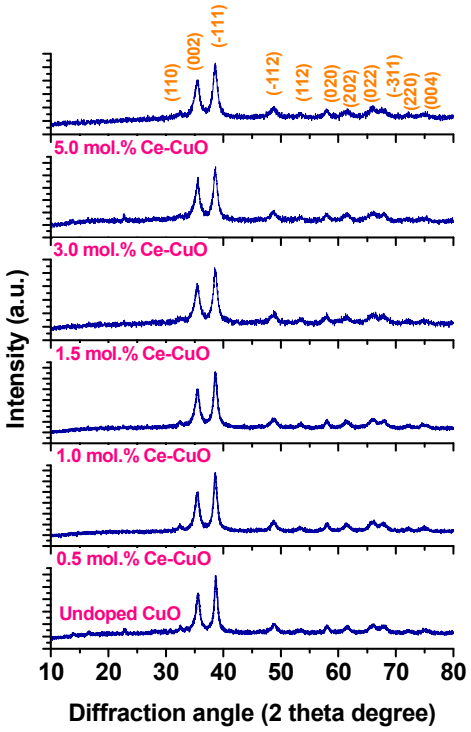

Figure 1. *XRD patterns of undoped and Ce-doped CuOsamples.*

A close observation of diffraction Ce doped CuO within the diffraction angle ranging from 2θ = 30-40°C (shown in Figure 2), indicates that the diffraction for (002) and (-111) planes of Ce doped CuO samples were slightly shifted to lower angles compared to those of undoped CuO. The shift towards lower angles was increased with increasing concentration of Ce^{3+} doping contents.

The observed change in lattice constant by increasing Ce contents can be attributed to difference in ionic radii of dopant Ce^{3+} (1.034A°) [29, 30] and host Cu^{2+} (0.73A°) [31]. These results further confirmed the substitution of Cu^{2+} ions by Ce^{3+} and successful doping of Ce^{3+} ions into the host matrix [32].

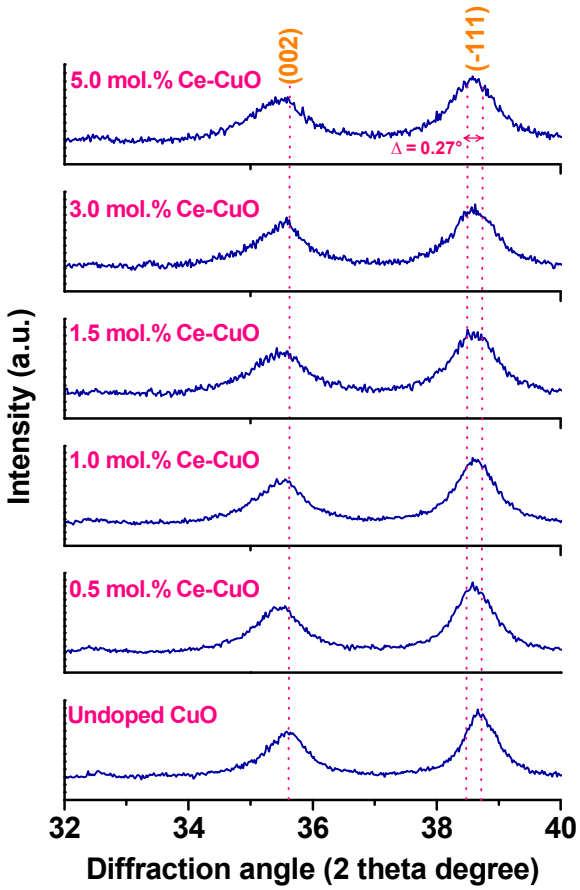

Figure 2. *Magnified view of (002) and (-111) diffraction peaks of undoped and Ce-doped CuO nanocomposites.*

3.2. FESEM Analysis

The microstructure and morphology of as-synthesized undoped and Ce doped CuO nanocomposites were further analyzed by FESEM analysis. Low and high magnification images of as-synthesized products are shown in Figure 3. As can be seen from the FESEM results, the undoped and Ce doped CuO samples exhibits nearly identical morphology. These consist of vesicular morphology having dimensions in the range of 50-100 nm. The surface of these composites is rough. Additionally, it can be observed that there is no change in size of CuO nanocomposites upto 3.0 mol.% Ce doping concentration, exceeding which agglomerated structures are observed to be formed.

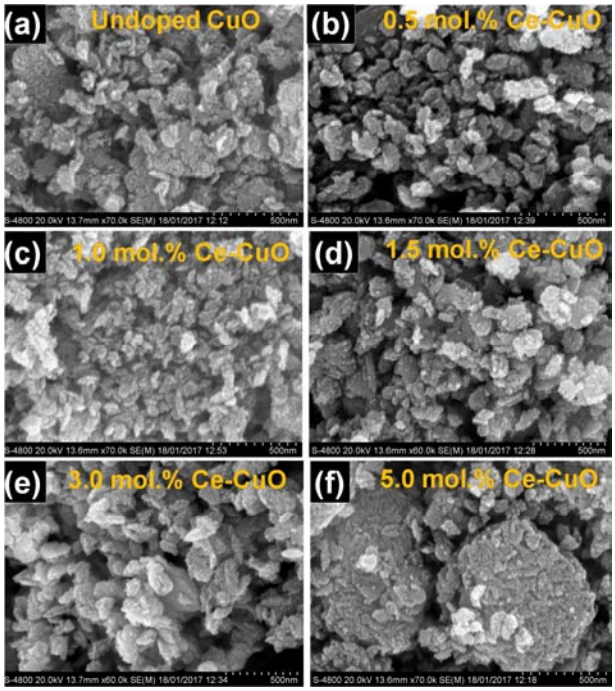

Figure 3. *Low and high magnification images of undoped and Ce-doped CuO nanocomposites.*

3.3. UV-Visible Absorption Spectra Analysis

The UV-visible absorption spectra of as-synthesized undoped and Ce doped CuO nanocomposites are shown in Figure 4. From figure all the as-synthesized composites shows a weak absorption peak in UV region in between 200-250 nm. However, the absorption in the visible region was high for all the as-synthesized nanocomposites. Additionally, it can also be observed that, as the Ce doping concentration increases the intensity of visible light absorption also increases. These results further indicate that as-synthesized nanocomposites can be used for photodegradation making use of sunlight.

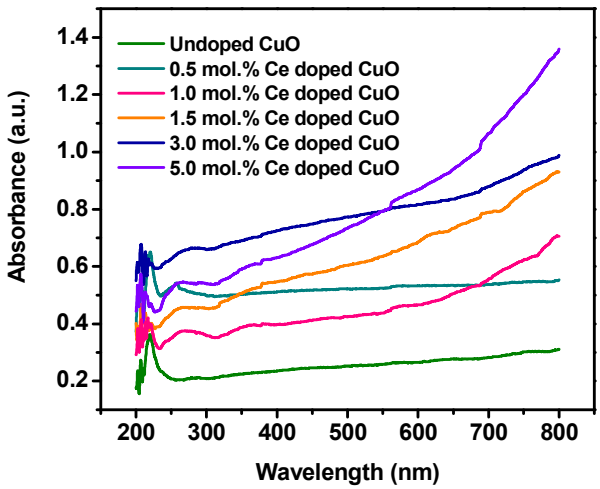

Figure 4. *UV-visible absorption spectra of undoped and Ce-doped CuO nanocomposites with different Ce^{3+} doping concentration (0.5–5.0mol.%).*

3.4. Photocatalytic Activity

In present study, the photocatalytic activities of as-synthesized CuO and Ce-CuO nanocomposites was studied using MB dye as test contaminant. Figure 5 depicts changes in absorption spectra of MB dye during photodegradation in presence of 3.0 mol.% Ce doped CuO nanocomposites. It can be seen from figure that, the intense absorption maxima at 664 nm corresponding to MB having intensity 1.79 a.u. decreases slowly with the sunlight irradiation time and completely diminished within approximately 180-200 mins.

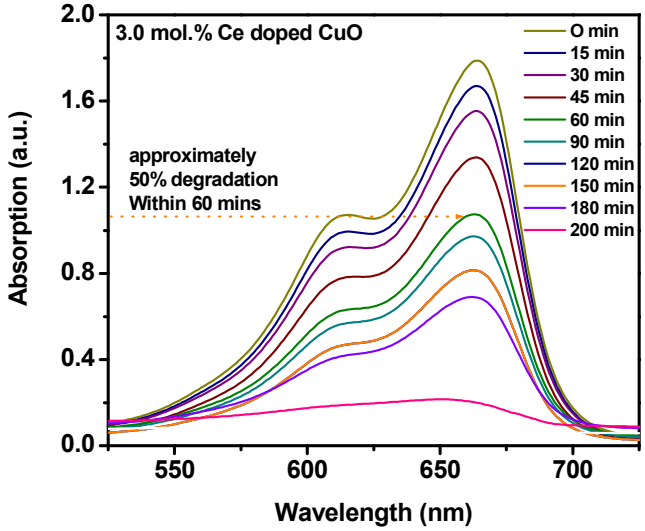

Figure 5. *UV-visible absorption spectra changes of MB dye during photodegradation in presence of 3.0 mol.% Ce-CuO catalysts.*

Figure 6 shows the curves for MB dye degradation with different as-synthesized catalysts. As can be seen from figure, in absence of any catalyst for blank experiment, MB dye washardly degraded. The degradation performance was achieved in presence of catalysts. Undoped CuO hardly degraded 49% of initial MB dye within 180 mins. The MB dye degradation was improved with Ce doped CuO catalysts and 3.0 mol.% Ce-CuO exhibited the highest degradation efficiency capable of degrading 98% MB dye within 180 mins.

Gradual decomposition of MB dye evident from Figure 5 suggests the slow degradation of MB dye molecules over the surface of as-synthesized CuO and Ce-CuO catalysts. The enhanced degradation in presence of Ce doped CuO catalysts can be attributed to the dopant Ce^{3+}. During photodegradation, the Ce^{3+} ions present in the CuO lattice can get oxidized to Ce^{4+} by releasing electrons which can further lead to formation of superoxide radicals (O_2^-) by reacting with adsorbed O_2. The oxidized Ce^{4+} species can act as electron scavenger or acceptor to trap photoexcited electrons from conduction band (CB) of CuO and consequently reduced to Ce^{3+}. Thus, the electron (e^-)-hole (h^+) recombination can be greatly reduced leading to enhanced photocatalytic activities.

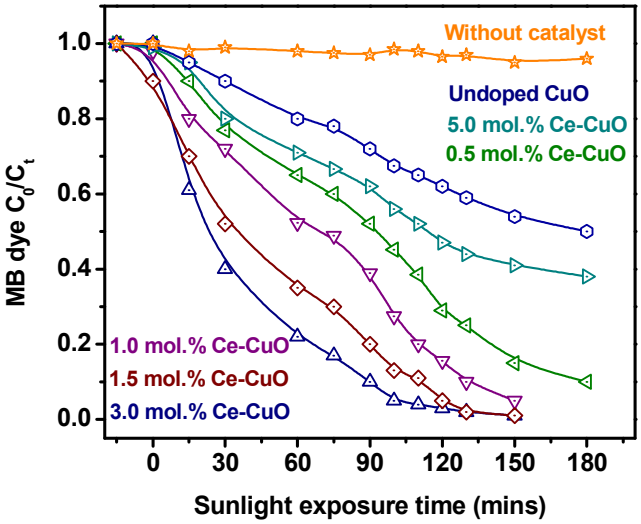

Figure 6. *Extents of MB dye degradation in presence of different as-synthesized catalysts under sunlight irradiation.*

The data of photodegradation experiments were further studied for MB dye degradation kinetics. The kinetics of MB dye degradation by as-synthesized catalysts can be described by pseudo first-order kinetics.

$$\mathrm{Ln}(C_0/C_t)=K_{app.}Xt \qquad (1)$$

Where; K_{app} is the apparent rate constant (min^{-1}), C_0 is the initial MB dye concentration and C_t is the MB dye concentration at sunlight exposure time t. The values for K_{app} can be calculated by extrapolating a linear fitting to the natural logarithm (C_0/C_t) versus the corresponding irradiation time and the results are presented in Figure 7.

From figure, it is evident that, the MB dye degradation rates increases with increasing concentrations of Ce^{3+} ion doping concentration. The order of rate constants follows the order; 3.0 mol.% Ce-CuO > 1.5 mol.% Ce-CuO > 1.0 mol.% Ce-CuO > 0.5 mol.% Ce-CuO > 5.0 mol.% Ce-CuO > undoped CuO. For 3.0 mol.% Ce-CuO nanocomposite, the degradation rate was maximum.

Repeated use of a catalyst while maintaining a constant activity determines the practical applicability of a catalyst. Therefore, the stability of catalyst to maintain constant activity over repeated use is an important criterion. Herein, present study the stability of photocatalytic activity was also studied by re-use of catalyst (3.0 mol% Ce-CuO) in fresh MB solution under sunlight irradiation. Figure 8 shows the degradation extent for consecutive four cycles using 3.0mol.% Ce-CuO (80 min sunlight irradiation for each cycle). As can be seen from figure, during first reuse, 98.0% of MB was degraded by 3.0 mol.% Ce-CuO. With subsequent reuse, the extent of MB dye degradation decreased to 94.0% and 91.0% for second and third recycles respectively. The decreased photocatalytic activity of 3.0mol.% Ce-CuO to some extent after every recycle can be considered due to handling losses of photocatalyst.

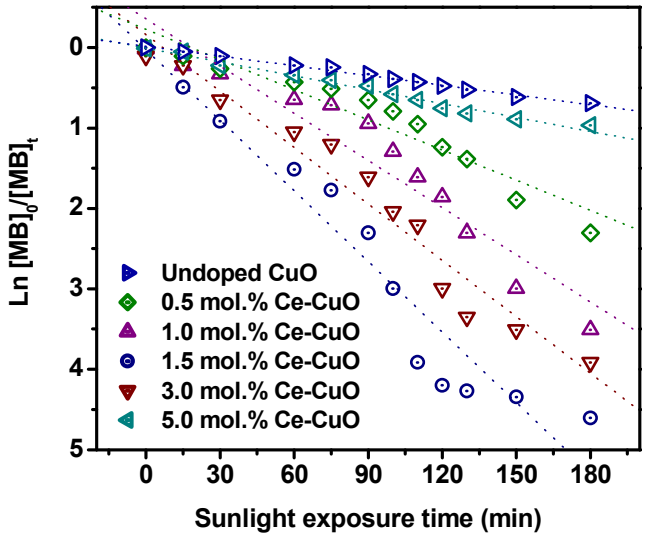

Figure 7. Apparent reaction rate constant (K_{app}) for undoped and Ce doped CuO catalysts.

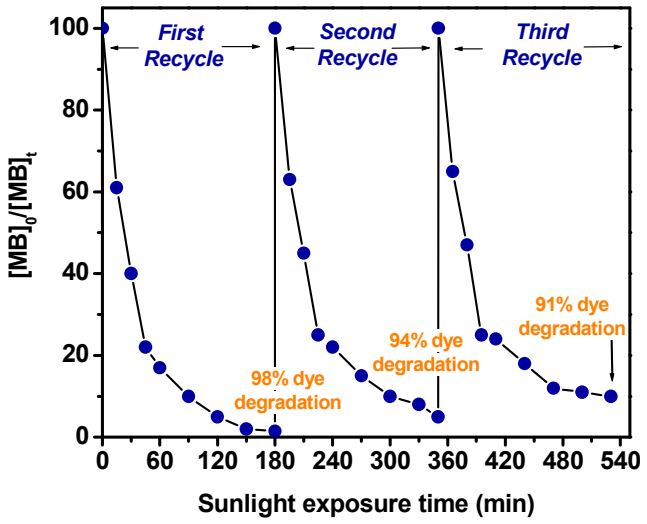

Figure 8. Recycle photocatalytic degradation performance of 3.0 mol.% Ce-CuO nanocomposite {[MBdye]=100ppm, 100mL; catalyst dose = 50mg; irradiation time = 180mins.}.

4. Conclusion

Ce^{3+} doped CuO catalysts were prepared by PEG-200 assisted facile sonochemical method. The as-synthesized nanocomposites are having vesicular morphology belonging to monoclinic CuO structures. The absorption intensities were found to increase with the increasing Ce^{3+} ion doping concentrations. Ce^{3+} doped CuO nanocomposites exhibited improved photocatalytic activities for degradation of MB dye under sunlight irradiation. 3.0 mol.% Ce-CuO exhibited the highest photocatalytic activity for MB degradation leading to 98% degradation within 180 mins, among the tested catalysts. These results further suggest potential candidature of as-synthesized catalysts for degradation of organic contaminants.

References

[1] O. Ozdemir, B. Armagan, M. Turan, M. S. Celik, Comparison of the adsorption characteristics of azo-reactive dyes on mesoporous minerals, Dyes Pigm. 62 (2004) 49–60.

[2] A. A. Ismail, T. A. Kandiel, D. W. Bahnemann, Novel (and better?) titania based photocatalysts: brookite nanorods and mesoporous structures, J. Photochem Photobiol: A Chem 216 (2010) 183–193.

[3] M. Alvaro, B. Cojocaru, A. A. Ismail, N. Petrea, B. Ferrer, F. A. Harraz, V. I. Parvulescu, H. Garcia, Visible-light photocatalytic activity of gold nanoparticles supported on template-synthesized mesoporous titania for the decontamination of the chemical war fare agent SOMAN, Appl. Catal. B 99 (2010) 191–197.

[4] S. Wang, H. Li, S. Xie, S. Liu, L. Xu, Physical and chemical regeneration of zeolitic adsorbents for dye removal in waste water treatment, Chemosphere 65 (2006) 82–87.

[5] A. A. Ismail, Facile synthesis of mesoporous Ag-loaded TiO_2 thin film and its photocatalytic properties, Microporous Mesoporous Mater. 159 (2012) 69–75.

[6] P. P. Selvam, S. Preethi, P. Basakaralingam, N. Thinakaran, A. Sivasamy, S. Sivanesan, Removal of rhodamine B from aqueous solution by adsorption onto sodium montmorillonite, J. Hazard. Mater. 155 (2008) 39–44.

[7] L. Bilińska, M. Gmurek, S. Ledakowicz, Textile waste water treatment by AOPs for brine reuse, Process Saf. Environ. Prot. 109 (2017) 420-428.

[8] M. E. (Bette) Meek, AOPs in hazard characterization for human health, Current Opinion in Toxicology, 3 (2017) 80-86.

[9] Kashif Nadeem, Gokce Tezcanli Guyer, Nadir Dizge, Polishing of biologically treated textile waste water through AOPs and recycling for wet processing, Journal of Water Process Engineering, 20 (2017) 29-39.

[10] Lucyna Bilińska, Marta Gmurek, Stanisław Ledakowicz, Comparison between industrial and simulated textile waste water treatment by AOPs–Biodegradability, toxicity and cost assessment, Chem. Eng. J., 306 (2016) 550-559.

[11] M. H. H. Mahamoud, A. A. Ismail, M. S. S. Sanad, Developing a cost-effective synthesis of iron oxide doped titania photocatalysts loaded with palladium, platinum or silver nanoparticles, Chem. Eng. J. 187 (2012) 96–103.

[12] M. A. Fox, M. T. Dulay, Heterogeneous photocatalysis, Chem. Rev. 93 (1993) 341–357.

[13] T. A. Kandiel, A. A. Ismail, D. W. Bahnemann, Mesoporous TiO_2 nanostructures: a route to minimize Pt loading on titania photocatalysts for hydrogen production, Phys Chem. Chem. Phys. 12 (2011) 20155–20161.

[14] J. Liu, C. Zhang, B. Ma, T. Yang, X. Gu, X. Wang, J. Zhang, C. Hu, Rational design of photoelectron-trapped / accumulated site and transportation path for superior photocatalyst, Nano Energy, 38 (2017) 271-280.

[15] A. B. Kuzmenko, D. vander Marel, P. J. M. vanBentum, E. A. Tishchenko, C. Presura, A. A. Bush, Phys. Rev. B 63 (2001) 094303.

[16] C. Dong, X. Xiao, G. Chen, H. Guan, Y. Wang, Appl. Surf. Sci. 349 (2015) 844–848.

[17] J. Demel, A. Zhigunov, I. Jirka, M. Klementová, K. Lang, J. Coll. Interf. Sci. 452 (2015) 174–179.

[18] T. Jiang, Y. Wang, D. Meng, M. Yu, Superlatt. Microst. 85 (2015) 1–6.

[19] Y. Wang, T. Jiang, D. Meng, H. Jin, M. Yu, Appl. Surf. Sci. 349 (2015) 636–643.

[20] A. Nezamzadeh-Ejhieh, M. Amiri, CuO supported clinoptilolite towards solarphotocatalytic degradation of p-aminophenol, Pow. Tech. 235 (2013) 279-288.

[21] Y. Zhang, J. He, R. Shi, P. Yang, Preparation and photofenton-like activities of high crystalline CuO fibers, Appl. Surf. Sci., 422 (2017) 1042-1051.

[22] A. Tadjarodi, O. Akhavan, K. Bijanzad, Photocatalytic activity of CuO nanoparticles incorporated in mesoporous structure prepared from bis (2-aminonicotinato) copper (II) microflakes, Transactions of Non ferrous Metals Society of China, 25 (2015) 3634-3642.

[23] W. Zhang, Z. Y. Zhong, Y. S. Wang, R. Xu, Doped solids olution: $(Zn_{0.95}Cu_{0.05})_{1-x}Cd_xS$ nanocrystals with high activity for H_2 evolution from aqueous solutions under visible light, J. Phys. Chem. C 112 (2008) 17635–17642.

[24] S. G. Yang, T. Li, B. X. Gu, Y. W. Du, H. Y. Sung, S. T. Hung, C. Y. Wong, A. B. Pakhomov, Appl. Phys. Lett. 83 (2003)18.

[25] R. A. Borzi, S. J. Stewart, G. Punte, R. C. Mercader, J. Appl. Phys. 87 (2000)9.

[26] S. Manna, S. K. De, J. Magn. Magn. Mater. 322 (2010) 2749–2753.

[27] Y. X. Li, M. Xu, L. Q. Pan, Y. P. Zhang, Z. G. Guo, C. Bi, J. Appl. Phys. 107 (2010) 113908.

[28] Mingyan Chuai, Qi Zhao, Tianye Yang, Yang Luo, Mingzhe Zhang, Synthesis and ferromagnetism study of Ce doped CuO dilute magnetic semiconductor, Materials Letters, 15 (2015) 205–207.

[29] Powder Diffract File, JCPDS-ICDD, 12 Campus Boulevard, Newtown Square, PA19073-3273, USA (2001).

[30] C. J. Chang, C. Y. Lin, J. K. Chen, M. H. Hsu, Ceram. Int. 40 (2014) 10867–10875.

[31] M. Faisal, A. A. Ismail, A. A. Ibrahim, H. Bouzid, S. A. Al-Sayari, Chem. Eng. J. 229 (2013) 225–233.

[32] Y. Wang, T. Jiang, D. Meng, D. Wang, M. Yu, Appl. Surf. Sci. 355 (2015) 191–196.

[33] T. Jan, J. Iqbal, Q. Mansoor, M. Ismail, M. S. H. Naqvi, A. Gul, S. F. H. Naqvi, F. Abbas, J. Phys. D: Appl. Phys. 47 (2014) 355301.